

## LST-1 observations of an enormous flare of BL Lacertae in 2021

---

**Seiya Nozaki,<sup>a,\*</sup> Katsuaki Asano,<sup>b</sup> Juan Escudero,<sup>c</sup> Gabriel Emery<sup>d</sup> and  
Chaitanya Priyadarshi<sup>e</sup> on behalf of the CTA-LST Project**

<sup>a</sup>Max-Planck-Institut für Physik, Föhringer Ring 6, 80805 München, Germany

<sup>b</sup>Institute for Cosmic Ray Research, University of Tokyo, 5-1-5, Kashiwa-no-ha, Kashiwa, Chiba 277-8582, Japan

<sup>c</sup>Instituto de Astrofísica de Andalucía-CSIC, Glorieta de la Astronomía s/n, 18008, Granada, Spain

<sup>d</sup>Aix Marseille Univ, CNRS/IN2P3, CPPM, Marseille, France

<sup>e</sup>Institut de Física d'Altes Energies (IFAE), The Barcelona Institute of Science and Technology, Campus UAB, 08193 Bellaterra (Barcelona), Spain

E-mail: [nozaki@mpp.mpg.de](mailto:nozaki@mpp.mpg.de)

The first prototype of LST (LST-1) for the Cherenkov Telescope Array has been in commissioning phase since 2018 and already started scientific observations with the low energy threshold around a few tens of GeV. In 2021, LST-1 observed BL Lac following the alerts based on multi-wavelength observations and detected prominent gamma-ray flares. In addition to the daily flux variability, LST-1 also detected sub-hour-scale intra-night variability reaching 3–4 times higher than the gamma-ray flux from the Crab Nebula above 100 GeV. In this proceeding, we will report the analysis results of LST-1 observations of BL Lac in 2021, especially focusing on flux variability.

38th International Cosmic Ray Conference (ICRC2023)  
26 July - 3 August, 2023  
Nagoya, Japan



---

\*Speaker

## 1. Introduction

Blazars are a type of active galactic nuclei (AGN) characterized by the presence of collimated relativistic plasma jets oriented toward the Earth. The emission from blazars is characterized by a highly variable non-thermal electromagnetic spectrum from radio to very-high-energy gamma rays (VHE;  $E > \sim 20$  GeV). The broadband SED has a two-hump structure. The lower-energy hump has a peak located from the radio to X-ray band and it is explained by the synchrotron emission from the accelerated leptons in the jet. On the other hand, the origin of the higher-energy hump located at gamma-ray bands is still under debate. Possible scenarios of the origin are inverse Compton scattering on low-energy photons emitted by synchrotron radiation and/or external photons (e.g. broad line region, dust torus). Blazars with no or faint optical emission lines are classified as "BL Lac" type object. In addition, it is sub-classified based on the peak frequency of the synchrotron peak ( $\nu_s$ ).

BL Lacertae (hereafter BL Lac) is a well-studied blazar located at redshift  $z = 0.069$  [1]. BL Lac is eponymous of the intermediate-synchrotron-peak "BL Lac" type object ( $10^{14}$  Hz  $< \nu_s < 10^{15}$  Hz) [2]. It is well known for the flux variability in various energy bands as described in [3]. In the VHE gamma-ray band, BL Lac is only detected during the flaring state so far. After the first detection in VHE gamma-ray band (above 1 TeV) in 1998 [4], MAGIC and VERITAS detected multiple flares of BL Lac with various flux levels [5–8]. Some observations also detected intra-night flux variability. As an example, VERITAS detected a decay time of  $13 \pm 4$  min in 2011 [6] and a rise and decay time of 2.3 hours and 36 minutes in 2016, respectively [8]. Since 2019, BL Lac was relatively active in the gamma-ray band and VHE gamma-ray flares were detected by MAGIC several times [9–11].

Cherenkov Telescope Array<sup>1</sup> (CTA) will be a next-generation very-high-energy gamma-ray observatory. Three different sizes of telescopes are planned to be built to cover a wide energy range with an order of magnitude better sensitivity than the current generation of Cherenkov telescopes. The Large-Sized Telescope<sup>2</sup>, with a 23-m diameter mirror dish, is designed to detect (relatively) low-energy signals, upwards from a few tens of GeV. The first prototype of LST (LST-1) was inaugurated at the CTA northern site (La Palma, Spain) in October 2018 and it has been in the commissioning phase. In parallel with the commissioning tests, LST-1 already started to observe gamma-ray objects for scientific purposes.

In this contribution, we present the analysis results of the LST-1 observations of an enormous flare of BL Lac in 2021.

## 2. LST observations and analysis

LST-1 started a campaign of BL Lac observations in July 2021 following the detection of the highest flux ever observed in the optical band [12]. On July 11 (MJD 59406), LST-1 detected VHE gamma-ray signals from BL Lac despite under bad weather conditions [13]. In August 2021, BL Lac was still active and VHE gamma-ray signals were also detected by MAGIC telescopes [14]. LST-1 continued its observation campaign until the mid of August 2021.

<sup>1</sup><https://www.cta-observatory.org/>

<sup>2</sup><https://www.lst1.iac.es/>

**Table 1:** LST observation conditions.

Date	MJD	Observation time [hours]	$Zd$ range [degrees]
Aug 3	59428.95–59429.05	1.76	20–45
Aug 4	59429.94–59430.13	1.92	14–49
Aug 5	59431.10–59431.13	0.50	14–16
Aug 6	59431.92–59431.95	0.55	44–51
Aug 8	59434.20–59434.22	0.44	34–41
Aug 9	59434.99–59435.09	1.93	14–32
Aug 10	59436.04–59436.10	1.34	13–19
Aug 12	59438.12–59438.17	0.92	19–30
Aug 13	59439.03–59439.05	0.45	15–20

The LST observations of BL Lac were performed during moonless time. We limited our observations to time windows with the source located at less than  $\sim 50$  degrees away from the zenith. It allows to take advantage of the LST-1 low-energy performance since low-energy photons are more absorbed by the thicker atmosphere crossed at lower altitudes. Each observation run takes 15–20 minutes. The total observation durations were 4.9 and 12.6 hours in July and August, respectively. We selected good-quality data based on the camera-averaged rate of pixel pulses with charge above 30 p.e as performed in [15] representing the quality of the atmospheric conditions. After the data selection, most of the LST-1 data taken in July 2021 were not selected. Thus, we only use the August datasets in this contribution and the duration of the selected August dataset is 9.8 hours. The observation of each night is summarized in Table 1.

The selected data were processed using the standard pipeline `cta-lstchain`<sup>3</sup> [16, 17]. The detail of the analysis procedures is described in [15]. In this contribution, we performed the analysis using a likelihood technique<sup>4</sup>, of which an earlier version is covered in [18], to parameterize the data instead of the Hillas’ parameters extraction used in [15]. The method performs a fit of a space-time signal model at the waveform level. The choice was also made to perform a so called source-dependent analysis, with the assumption of the knowledge of the source position being used in the event reconstruction. For the gamma-like event selection, we use *alpha* (angle between shower axis and the line between the known source position and the image centroid) and *gammaness* (the score indicating how likely it is that the primary particle is a gamma ray) obtained by machine learning. In addition, we apply an event cut of *intensity* (the sum of the charges of the pixels which survive the image cleaning) above 50 photo-electrons to ensure the data quality. The instrumental response function (IRF) of Cherenkov telescopes depends on the pointing direction of the telescope. Thus, we compute the IRF by the interpolation of ones obtained with the simulation data at different pointing directions. The high level analysis was performed using `gammapy`<sup>5</sup> [19, 20] to find the best spectral model using likelihood ratio test and compute the integrated gamma-ray flux.

<sup>3</sup><https://github.com/cta-observatory/cta-lstchain>

<sup>4</sup>available in `cta-lstchain` v0.9.7+

<sup>5</sup><https://github.com/gammapy/gammapy>

### 3. Multi-wavelength observations and analysis

#### 3.1 Fermi-LAT

The Large Area Telescope (LAT) on board the *Fermi* Gamma-ray Space Telescope is a wide field-of-view pair-conversion telescope covering the energy range from below 20 MeV to more than 300 GeV [21]. It has a wide field of view so that the entire sky is scanned every three hours for the standard survey mode. We analyzed *Fermi*-LAT data between July 29, 2021 (MJD=59424) and August 15, 2021 (MJD=59441) covering the LST-1 observation periods in August 2021. We performed the binned likelihood analysis using `fermipy`<sup>6</sup>. The analysis settings follow the recommendation for the Pass 8 data analysis<sup>7</sup>. We analyzed the data in 24-hours and 12-hours bins.

#### 3.2 Swift-UVOT, XRT

The Neil Gehrels *Swift* Observatory is a multiwavelength mission for Gamma-Ray Burst astronomy and has been operational since 2004 [22]. *Swift* carried out 13 observations of BL Lac around the LST-1 observation campaign in August 2021. In this proceeding, we used the data obtained by the X-ray Telescope (XRT) [23] (0.2–10.0 keV) and the Ultraviolet/Optical Telescope (UVOT) [24] (170–600 nm) onboard the *Swift* satellite. XRT data were processed using an online XRT product generator<sup>8</sup> and UVOT data were analyzed using the python wrapper tool including the official UVOT analysis pipeline<sup>9,10</sup>

## 4. Results

#### 4.1 VHE gamma-ray signal detection

Fig. 1 shows the distribution of  $\alpha$  from the expected source position (ON) and another position without gamma-ray sources (OFF) on Aug 9. The VHE gamma-ray signals are clearly detected with a significance of  $43.4\sigma$ . The background level at a larger  $\alpha$  region is consistent between ON and OFF events. Even though the difference in the background level is small, it can significantly affect the results at the lowest energy range since the background rejection power of the single telescope data analysis is worse than the stereo data analysis below  $\sim 100$  GeV as seen in Fig. 16 of [15]. For this flare, the signal-to-noise ratio is high even for the low-energy events so that the results are less affected by the background normalization factors than other gamma-ray sources.

#### 4.2 VHE gamma-ray light curve

Fig. 2 shows the intra-night light curve above 100 GeV on Aug 9. The flux level was variable during this night and reached 3–4 times higher than that of the Crab Nebula (Crab Unit; C.U.) at maximum. Two peaks can be seen in the intra-night light curve, both with a rise and decay time scale around 10–20 minutes.

<sup>6</sup><https://github.com/fermiPy/fermipy>

<sup>7</sup>[https://fermi.gsfc.nasa.gov/ssc/data/analysis/documentation/Pass8\\_usage.html](https://fermi.gsfc.nasa.gov/ssc/data/analysis/documentation/Pass8_usage.html)

<sup>8</sup>[https://www.swift.ac.uk/user\\_objects/](https://www.swift.ac.uk/user_objects/)

<sup>9</sup><https://www.swift.ac.uk/analysis/uvot/>

<sup>10</sup><https://github.com/KarlenS/swift-uvot-analysis-tools>

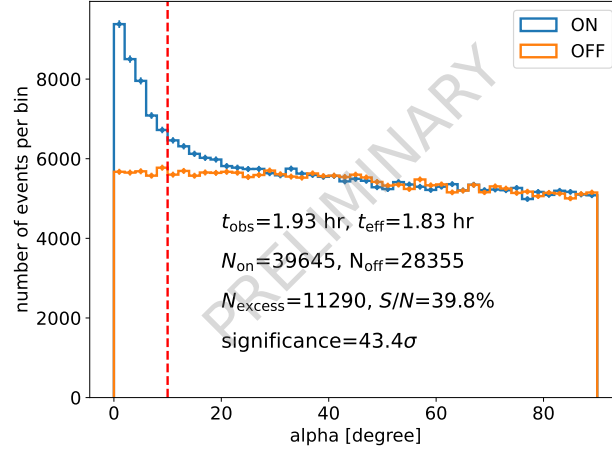


**Figure 1:** Distributions of  $\alpha$  of the LST observation on Aug 9. Blue and orange histograms correspond to the distribution of ON and OFF events, respectively. Each error bar shows the statistical uncertainty. Here, we apply event cuts of  $\text{intensity} > 50$  p.e. and  $\text{gammaness} > 0.9$ . To compute the statistics in the figure, a cut of  $\alpha < 10$  degrees (red-dashed line) is also applied.

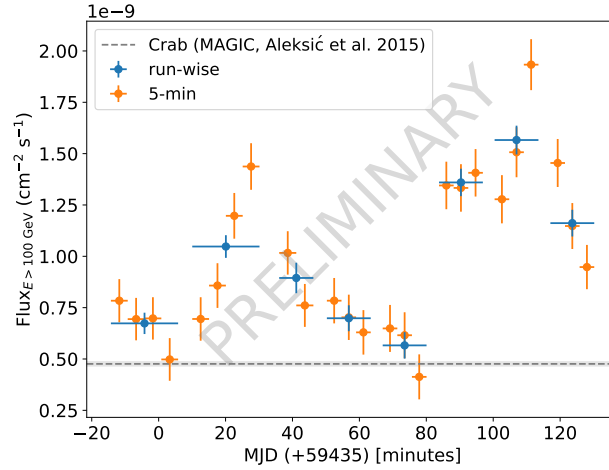


**Figure 2:** Intra-night light curve ( $>100$  GeV) observed by the LST-1 on Aug 9. Blue and orange points correspond to run-wise and 5-min duration. The error bars on the flux level show statistical uncertainties. The gray line shows the integral flux of the Crab Nebula obtained by the MAGIC [25] as a reference.

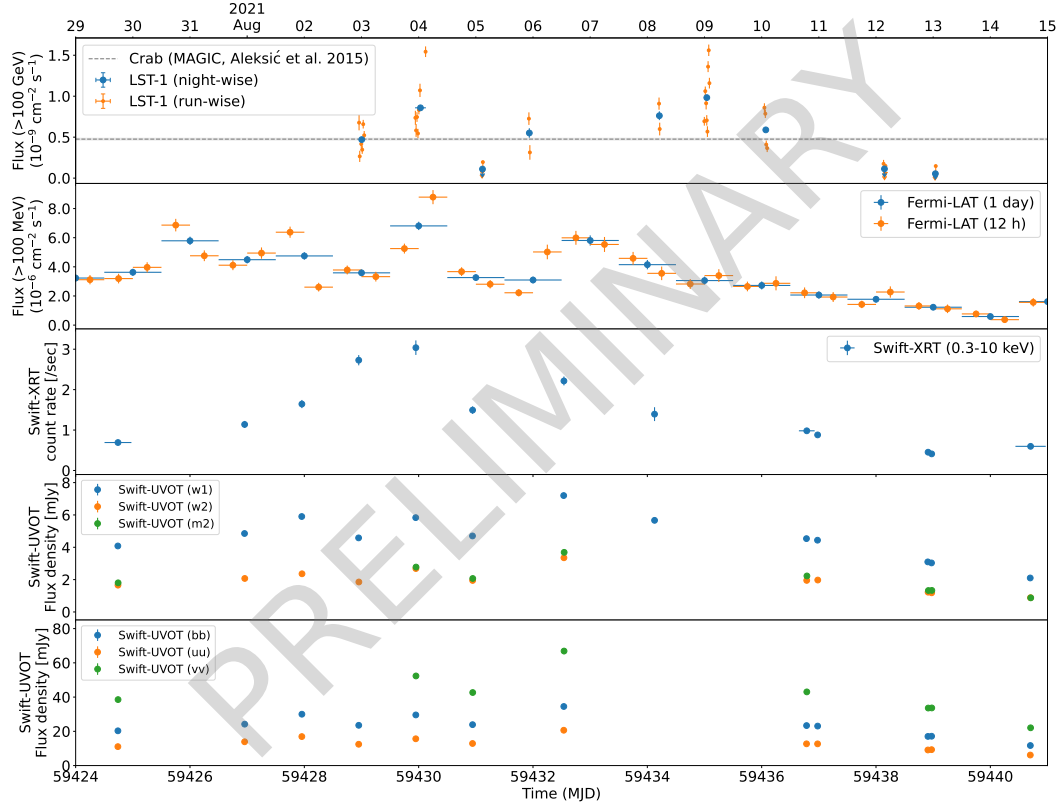


**Figure 3:** Multi-wavelength light curves of the BL Lacertae between MJD=59424 and 59441 (VHE gamma-ray: LST-1 (>100 GeV), high-energy gamma-ray: Fermi-LAT (> 100 MeV), X-ray: Swift-XRT (0.3–10 keV), Ultraviolet and Optical: Swift-UVOT). For LST-1, night-wise (blue) and run-wise (orange) light curves are shown. Gray dashed line shows the integral flux of the Crab Nebula [25] as shown in Fig. 2. For Fermi-LAT, 1-day (blue) and 12-day (orange) light curves are shown.

### 4.3 Multi-wavelength light curve

Fig. 3 shows the multi-wavelength light curve around the LST-1 observation period. In the night-wise LST light curve, we can see the flux variation ( $<0.1$ – $2$  C.U.) on a long time scale with large intra-night variabilities. In the *Fermi*-LAT light curve, multiple peaks were detected during this period and the highest flux was observed around Aug 4 when LST-1 also detected high flux ( $\sim 3$  C.U.) in the run-wise light curve. Around this peak, Swift-XRT also detected the highest count rates reaching around three times higher than the lowest rates during this period. After all of the bands showed an increase in the flux again around Aug 6–7, it gradually decreased except for the LST-1 data points observed on Aug 9.

## 5. Summary

LST-1 performed the observation of BL Lac flare in 2021. During the observation campaign, VHE gamma-ray signals were detected on most nights and the detection significance was  $43.4\sigma$  on Aug 9 with the high signal-to-noise ratio. We have observed the intra-night variability with the flux level of 3–4 C.U. at the peak. This variability had a sub-hour scale double-peak structure. The LST-1 night-wise light curve also shows the daily-scale flux variability ( $<0.1$ – $2$  C.U.). *Fermi*-LAT and Swift-XRT show the highest flux around Aug 4 when LST-1 also detected a high flux of  $\sim 3$  C.U. in the run-wise light curve. The detailed discussion and interpretation will be described in a future paper.

## Acknowledgments

We gratefully acknowledge financial support from the following agencies and organisations: Conselho Nacional de Desenvolvimento Científico e Tecnológico (CNPq), Fundação de Amparo à Pesquisa do Estado do Rio de Janeiro (FAPERJ), Fundação de Amparo à Pesquisa do Estado de São Paulo (FAPESP), Fundação de Apoio à Ciência, Tecnologia e Inovação do Paraná - Fundação Araucária, Ministry of Science, Technology, Innovations and Communications (MCTIC), Brasil; Ministry of Education and Science, National RI Roadmap Project DOI-153/28.08.2018, Bulgaria; Croatian Science Foundation, Rudjer Boskovic Institute, University of Osijek, University of Rijeka, University of Split, Faculty of Electrical Engineering, Mechanical Engineering and Naval Architecture, University of Zagreb, Faculty of Electrical Engineering and Computing, Croatia; Ministry of Education, Youth and Sports, MEYS LM2015046, LM2018105, LTT17006, EU/MEYS CZ.02.1.01/0.0/0.0/16\_013/0001403, CZ.02.1.01/0.0/0.0/18\_046/0016007 and CZ.02.1.01/0.0/0.0/16\_019/0000754, Czech Republic; CNRS-IN2P3, the French Programme d'investissements d'avenir and the Enigmass Labex, This work has been done thanks to the facilities offered by the Univ. Savoie Mont Blanc - CNRS/IN2P3 MUST computing center, France; Max Planck Society, German Bundesministerium für Bildung und Forschung (Verbundforschung / ErUM), Deutsche Forschungsgemeinschaft (SFBs 876 and 1491), Germany; Istituto Nazionale di Astrofisica (INAF), Istituto Nazionale di Fisica Nucleare (INFN), Italian Ministry for University and Research (MUR); ICRR, University of Tokyo, JSPS, MEXT, Japan; JST SPRING - JPMJSP2108; Narodowe Centrum Nauki, grant number 2019/34/E/ST9/00224, Poland; The Spanish groups acknowledge the Spanish Ministry of Science and Innovation and the Spanish Research State Agency (AEI) through the government budget lines PGE2021/28.06.000X.411.01, PGE2022/28.06.000X.411.01 and PGE2022/28.06.000X.711.04, and grants PID2022-139117NB-C44, PID2019-104114RB-C31, PID2019-107847RB-C44, PID2019-104114RB-C32, PID2019-105510GB-C31, PID2019-104114RB-C33, PID2019-107847RB-C41, PID2019-107847RB-C43, PID2019-107847RB-C42, PID2019-107988GB-C22, PID2021-124581OB-I00, PID2021-125331NB-I00; the "Centro de Excelencia Severo Ochoa" program through grants no. CEX2019-000920-S, CEX2020-001007-S, CEX2021-001131-S; the "Unidad de Excelencia María de Maeztu" program through grants no. CEX2019-000918-M, CEX2020-001058-M; the "Ramón y Cajal" program through grants RYC2021-032552-I, RYC2021-032991-I, RYC2020-028639-I and RYC-2017-22665; the "Juan de la Cierva-Incorporación" program through grants no. IJC2018-037195-I, IJC2019-040315-I. They also acknowledge the "Atracción de Talento" program of Comunidad de Madrid through grant no. 2019-T2/TIC-12900; the project "Tecnologías avanzadas para la exploración del universo y sus componentes" (PR47/21 TAU), funded by Comunidad de Madrid, by the Recovery, Transformation and Resilience Plan from the Spanish State, and by NextGenerationEU from the European Union through the Recovery and Resilience Facility; the La Caixa Banking Foundation, grant no. LCF/BQ/PI21/11830030; the "Programa Operativo" FEDER 2014-2020, Consejería de Economía y Conocimiento de la Junta de Andalucía (Ref. 1257737), PAIDI 2020 (Ref. P18-FR-1580) and Universidad de Jaén; "Programa Operativo de Crecimiento Inteligente" FEDER 2014-2020 (Ref. ESFRI-2017-IAC-12), Ministerio de Ciencia e Innovación, 15% co-financed by Consejería de Economía, Industria, Comercio y Conocimiento del Gobierno de Canarias; the "CERCA" program and the grant 2021SGR00426, both funded by the Generalitat de Catalunya; and the European

Union's "Horizon 2020" GA:824064 and NextGenerationEU (PRTR-C17.I1). State Secretariat for Education, Research and Innovation (SERI) and Swiss National Science Foundation (SNSF), Switzerland; The research leading to these results has received funding from the European Union's Seventh Framework Programme (FP7/2007-2013) under grant agreements No 262053 and No 317446; This project is receiving funding from the European Union's Horizon 2020 research and innovation programs under agreement No 676134; ESCAPE - The European Science Cluster of Astronomy & Particle Physics ESFRI Research Infrastructures has received funding from the European Union's Horizon 2020 research and innovation programme under Grant Agreement no. 824064.

## References

- [1] J. S. Miller et al., 1978, *ApJ*, 219, L85
- [2] Ackermann M. et al., 2011, *ApJ*, 743, 171
- [3] N. Sahakyan and P. Giommi, 2022, *MNRAS*, 513, 4645
- [4] Y. I. Neshpor et al., 2001, *Astron. Rep.*, 45, 249
- [5] J. Albert et al., 2007, *ApJ*, 666, L17
- [6] T. Arlen et al., 2013, *ApJ*, 762, 92
- [7] MAGIC Collaboration et al., 2019, *A&A*, 623, A175
- [8] A. U. Abeysekara et al., 2018, *ApJ*, 856, 95
- [9] R. Mirzoyan (MAGIC collaboration), 2019, *The Astronomer's Telegram* 12724
- [10] O. Blanch (MAGIC collaboration), 2020, *The Astronomer's Telegram* 13963
- [11] O. Blanch (MAGIC collaboration), 2020, *The Astronomer's Telegram* 14032
- [12] R. M. Corcoran et al., 2021, *The Astronomer's Telegram* 14773
- [13] J. Cortina (CTA LST Project), 2021, *The Astronomer's Telegram* 14783
- [14] O. Blanch (MAGIC collaboration), 2021, *The Astronomer's Telegram* 14826
- [15] CTA-LST Project, 2023, *arXiv e-prints*, arXiv:2306.12960
- [16] R. L. Coto et al., cta-lstchain version 0.9.8 (2022 Oct), DOI:10.5281/zenodo.7243430
- [17] R. L. Coto et al., 2021, *Proc. of 37th Int. Cosmic Ray Conf.*, 395, 806
- [18] G. Emery et al., 2021, *Proc. of 37th Int. Cosmic Ray Conf.*, 395, 716
- [19] C. Deil et al., 2017, *Proc. of 35th Int. Cosmic Ray Conf.*, 301, 766
- [20] F. Acero et al., gammapy version 1.0 (2022 Nov), DOI:10.5281/zenodo.7311399
- [21] W. B. Atwood et al., 2009, *ApJ*, 697, 1071
- [22] N. Gehrels et al., 2004, *ApJ*, 611, 1005
- [23] D. N. Burrows et al., 2004, *Space Sci. Rev.*, 120, 165
- [24] P. W. A. Roming et al., 2005, *Space Sci. Rev.*, 120, 95
- [25] J. Aleksić et al., 2015, *JHEAP*, 5, 30



## Full Author List: CTA-LST project

K. Abe<sup>1</sup>, S. Abe<sup>2</sup>, A. Aguasca-Cabot<sup>3</sup>, I. Agudo<sup>4</sup>, N. Alvarez Crespo<sup>5</sup>, L. A. Antonelli<sup>6</sup>, C. Aramo<sup>7</sup>, A. Arbet-Engels<sup>8</sup>, C. Arcaro<sup>9</sup>, M. Artero<sup>10</sup>, K. Asano<sup>2</sup>, P. Aubert<sup>11</sup>, A. Baktash<sup>12</sup>, A. Bamba<sup>13</sup>, A. Baquero Larriva<sup>5,14</sup>, L. Baroncelli<sup>15</sup>, U. Barres de Almeida<sup>16</sup>, J. A. Barrio<sup>5</sup>, I. Batković<sup>9</sup>, J. Baxter<sup>2</sup>, J. Becerra González<sup>17</sup>, E. Bernardini<sup>9</sup>, M. I. Bernardos<sup>4</sup>, J. Bernete Medrano<sup>18</sup>, A. Berti<sup>8</sup>, P. Bhattacharjee<sup>11</sup>, N. Biederbeck<sup>19</sup>, C. Bigongiari<sup>6</sup>, E. Bissaldi<sup>20</sup>, O. Blanch<sup>10</sup>, G. Bonnoli<sup>21</sup>, P. Bordas<sup>3</sup>, A. Bulgarelli<sup>15</sup>, I. Burelli<sup>22</sup>, L. Burmistrov<sup>23</sup>, M. Buscemi<sup>24</sup>, M. Cardillo<sup>25</sup>, S. Caroffi<sup>11</sup>, A. Carosi<sup>6</sup>, M. S. Carrasco<sup>26</sup>, F. Cassol<sup>26</sup>, D. Cauz<sup>22</sup>, D. Cerasole<sup>27</sup>, G. Ceribella<sup>8</sup>, Y. Chai<sup>8</sup>, K. Cheng<sup>2</sup>, A. Chiavassa<sup>28</sup>, M. Chikawa<sup>2</sup>, L. Chytka<sup>29</sup>, A. Cifuentes<sup>18</sup>, J. L. Contreras<sup>5</sup>, J. Cortina<sup>18</sup>, H. Costantini<sup>26</sup>, M. Dalchenko<sup>23</sup>, F. Dazzi<sup>6</sup>, A. De Angelis<sup>9</sup>, M. de Bony de Lavergne<sup>11</sup>, B. De Lotto<sup>22</sup>, M. De Lucia<sup>7</sup>, R. de Menezes<sup>28</sup>, L. Del Peral<sup>30</sup>, G. Deleglise<sup>11</sup>, C. Delgado<sup>18</sup>, J. Delgado Mengual<sup>31</sup>, D. della Volpe<sup>23</sup>, M. Dellaiera<sup>11</sup>, A. Di Piano<sup>15</sup>, F. Di Piero<sup>28</sup>, A. Di Pilato<sup>23</sup>, R. Di Tria<sup>27</sup>, L. Di Venere<sup>27</sup>, C. Díaz<sup>18</sup>, R. M. Dominik<sup>19</sup>, D. Dominis Prester<sup>32</sup>, A. Donini<sup>6</sup>, D. Dorner<sup>33</sup>, M. Doró<sup>9</sup>, L. Eisenberger<sup>33</sup>, D. Elsässer<sup>19</sup>, G. Emery<sup>26</sup>, J. Escudero<sup>4</sup>, V. Fallah Ramazani<sup>34</sup>, G. Ferrara<sup>24</sup>, F. Ferraro<sup>35</sup>, A. Fiasson<sup>11,36</sup>, L. Foffano<sup>25</sup>, L. Freixas Coromina<sup>18</sup>, S. Fröse<sup>19</sup>, S. Fukami<sup>2</sup>, Y. Fukazawa<sup>37</sup>, E. García<sup>11</sup>, R. García López<sup>17</sup>, C. Gasbarra<sup>38</sup>, D. Gasparrini<sup>38</sup>, D. Geyer<sup>19</sup>, J. Giesbrecht Paiva<sup>16</sup>, N. Giglietto<sup>20</sup>, F. Giordano<sup>27</sup>, P. Gliwny<sup>39</sup>, N. Godinovic<sup>40</sup>, R. Grau<sup>10</sup>, J. Green<sup>8</sup>, D. Green<sup>8</sup>, S. Gunji<sup>41</sup>, P. Günther<sup>33</sup>, J. Hackfeld<sup>34</sup>, D. Hadasch<sup>2</sup>, A. Hahn<sup>8</sup>, K. Hashiyama<sup>2</sup>, T. Hassan<sup>18</sup>, K. Hayashi<sup>2</sup>, L. Heckmann<sup>8</sup>, M. Heller<sup>23</sup>, J. Herrera Llorente<sup>17</sup>, K. Hirotani<sup>2</sup>, D. Hoffmann<sup>26</sup>, D. Horns<sup>12</sup>, J. Houles<sup>26</sup>, M. Hrabovsky<sup>29</sup>, D. Hrupec<sup>42</sup>, D. Hui<sup>2</sup>, M. Hütten<sup>2</sup>, M. Iarlori<sup>43</sup>, R. Imazawa<sup>37</sup>, T. Inada<sup>2</sup>, Y. Inome<sup>2</sup>, K. Ioka<sup>44</sup>, M. Iori<sup>35</sup>, K. Ishio<sup>39</sup>, I. Jimenez Martinez<sup>18</sup>, J. Jurysek<sup>45</sup>, M. Kagaya<sup>2</sup>, V. Karas<sup>46</sup>, H. Katagiri<sup>47</sup>, J. Kataoka<sup>48</sup>, D. Kerszberg<sup>10</sup>, Y. Kobayashi<sup>2</sup>, K. Kohri<sup>49</sup>, A. Kong<sup>2</sup>, H. Kubo<sup>2</sup>, J. Kushida<sup>1</sup>, M. Lainez<sup>5</sup>, G. Lamanna<sup>11</sup>, A. Lamastra<sup>6</sup>, T. Le Flour<sup>11</sup>, M. Linhoff<sup>19</sup>, F. Longo<sup>50</sup>, R. López-Coto<sup>4</sup>, A. López-Oramas<sup>17</sup>, S. Loporchio<sup>27</sup>, A. Lorini<sup>51</sup>, J. Lozano Bahilo<sup>30</sup>, P. L. Luque-Escamilla<sup>52</sup>, P. Majumdar<sup>53,2</sup>, M. Makariev<sup>54</sup>, D. Mandat<sup>45</sup>, M. Manganaro<sup>32</sup>, G. Manicò<sup>24</sup>, K. Mannheim<sup>33</sup>, M. Mariotti<sup>9</sup>, P. Marquet<sup>10</sup>, G. Marsella<sup>24,55</sup>, J. Martí<sup>52</sup>, O. Martínez<sup>56</sup>, G. Martínez<sup>18</sup>, M. Martínez<sup>10</sup>, A. Mas-Aguilar<sup>5</sup>, G. Maurin<sup>11</sup>, D. Mazin<sup>2,8</sup>, E. Mestre Guillen<sup>52</sup>, S. Micanovic<sup>52</sup>, D. Miceli<sup>9</sup>, T. Miener<sup>5</sup>, J. M. Miranda<sup>56</sup>, R. Mirzoyan<sup>8</sup>, T. Mizuno<sup>57</sup>, M. Molero Gonzalez<sup>17</sup>, E. Molina<sup>3</sup>, T. Montaruli<sup>23</sup>, I. Monteiro<sup>11</sup>, A. Moralejo<sup>10</sup>, D. Morcuende<sup>5</sup>, A. Morselli<sup>38</sup>, V. Moya<sup>5</sup>, H. Murai<sup>58</sup>, K. Murase<sup>2</sup>, S. Nagataki<sup>59</sup>, T. Nakamori<sup>41</sup>, A. Neronov<sup>60</sup>, L. Nickel<sup>19</sup>, M. Nieves Rosillo<sup>17</sup>, K. Nishijima<sup>1</sup>, K. Noda<sup>2</sup>, D. Nosek<sup>61</sup>, S. Nozaki<sup>8</sup>, M. Ohishi<sup>2</sup>, Y. Ohtani<sup>2</sup>, T. Oka<sup>62</sup>, A. Okumura<sup>63,64</sup>, R. Orito<sup>65</sup>, J. Otero-Santos<sup>17</sup>, M. Palatiello<sup>22</sup>, D. Paneque<sup>8</sup>, F. R. Pantaleo<sup>20</sup>, R. Paoletti<sup>51</sup>, J. M. Paredes<sup>3</sup>, M. Pech<sup>45,29</sup>, M. Pecimotika<sup>32</sup>, M. Peresano<sup>28</sup>, F. Pfeiffle<sup>33</sup>, E. Pietropaolo<sup>66</sup>, G. Pirola<sup>8</sup>, C. Plard<sup>11</sup>, F. Podobnik<sup>31</sup>, V. Poireau<sup>11</sup>, M. Polo<sup>18</sup>, E. Pons<sup>11</sup>, E. Prandini<sup>9</sup>, J. Prast<sup>11</sup>, G. Principe<sup>30</sup>, C. Priyadarshi<sup>10</sup>, M. Prouza<sup>45</sup>, R. Rando<sup>9</sup>, W. Rhode<sup>19</sup>, M. Ribó<sup>3</sup>, C. Righi<sup>21</sup>, V. Rizi<sup>66</sup>, G. Rodríguez Fernández<sup>38</sup>, M. D. Rodríguez Frías<sup>30</sup>, T. Saito<sup>2</sup>, S. Sakurai<sup>2</sup>, D. A. Sanchez<sup>11</sup>, T. Sarić<sup>40</sup>, Y. Sato<sup>67</sup>, F. G. Saturni<sup>6</sup>, V. Savchenko<sup>60</sup>, B. Schleiher<sup>33</sup>, F. Schmuckermair<sup>8</sup>, J. L. Schubert<sup>19</sup>, F. Schussler<sup>68</sup>, T. Schweizer<sup>8</sup>, M. Seglar Arroyo<sup>11</sup>, T. Siegert<sup>33</sup>, R. Silva<sup>27</sup>, J. Sitarek<sup>39</sup>, V. Sliusar<sup>69</sup>, A. Spolon<sup>9</sup>, J. Strišković<sup>42</sup>, M. Strzys<sup>2</sup>, Y. Suda<sup>37</sup>, H. Tajima<sup>63</sup>, M. Takahashi<sup>63</sup>, H. Takahashi<sup>37</sup>, J. Takata<sup>2</sup>, R. Takeishi<sup>2</sup>, P. H. T. Tam<sup>2</sup>, S. J. Tanaka<sup>67</sup>, D. Tateishi<sup>70</sup>, P. Temnikov<sup>54</sup>, Y. Terada<sup>70</sup>, K. Terauchi<sup>62</sup>, T. Terzić<sup>32</sup>, M. Teshima<sup>8,2</sup>, M. Tluczykont<sup>12</sup>, F. Tokana<sup>41</sup>, D. F. Torres<sup>71</sup>, P. Travnicek<sup>45</sup>, S. Truzzi<sup>51</sup>, A. Tutone<sup>6</sup>, M. Vacula<sup>28</sup>, J. van Scherpenberg<sup>8</sup>, M. Vázquez Acosta<sup>17</sup>, I. Vial<sup>9</sup>, A. Vigliano<sup>22</sup>, C. F. Vigorito<sup>28,72</sup>, V. Vitale<sup>38</sup>, G. Voutsinas<sup>23</sup>, I. Vovk<sup>2</sup>, T. Vuillaume<sup>11</sup>, R. Walter<sup>69</sup>, Z. Wei<sup>71</sup>, M. Will<sup>8</sup>, T. Yamamoto<sup>73</sup>, R. Yamazaki<sup>67</sup>, T. Yoshida<sup>47</sup>, T. Yoshikoshi<sup>2</sup>, N. Zywuca<sup>39</sup>

<sup>1</sup>Department of Physics, Tokai University. <sup>2</sup>Institute for Cosmic Ray Research, University of Tokyo. <sup>3</sup>Departament de Física Quàntica i Astrofísica, Institut de Ciències del Cosmos, Universitat de Barcelona, IEEC-UB. <sup>4</sup>Instituto de Astrofísica de Andalucía-CSIC. <sup>5</sup>EMFTEL department and IPARCOS, Universidad Complutense de Madrid. <sup>6</sup>INAF - Osservatorio Astronomico di Roma. <sup>7</sup>INFN Sezione di Napoli. <sup>8</sup>Max-Planck-Institut für Physik. <sup>9</sup>INFN Sezione di Padova and Università degli Studi di Padova. <sup>10</sup>Institut de Física d'Altes Energies (IFAE), The Barcelona Institute of Science and Technology. <sup>11</sup>LAPP, Univ. Grenoble Alpes, Univ. Savoie Mont Blanc, CNRS-IN2P3, Annecy. <sup>12</sup>Universität Hamburg, Institut für Experimentalphysik. <sup>13</sup>Graduate School of Science, University of Tokyo. <sup>14</sup>Universidad del Azuay. <sup>15</sup>INAF - Osservatorio di Astrofisica e Scienza dello spazio di Bologna. <sup>16</sup>Centro Brasileiro de Pesquisas Físicas. <sup>17</sup>Instituto de Astrofísica de Canarias and Departamento de Astrofísica, Universidad de La Laguna. <sup>18</sup>CIEMAT. <sup>19</sup>Department of Physics, TU Dortmund University. <sup>20</sup>INFN Sezione di Bari and Politecnico di Bari. <sup>21</sup>INAF - Osservatorio Astronomico di Brera. <sup>22</sup>INFN Sezione di Trieste and Università degli Studi di Udine. <sup>23</sup>University of Geneva - Département de physique nucléaire et corpusculaire. <sup>24</sup>INFN Sezione di Catania. <sup>25</sup>INAF - Istituto di Astrofisica e Planetologia Spaziali (IAPS). <sup>26</sup>Aix Marseille Univ, CNRS/IN2P3, CPPM. <sup>27</sup>INFN Sezione di Bari and Università di Bari. <sup>28</sup>INFN Sezione di Torino. <sup>29</sup>Palacky University Olomouc, Faculty of Science. <sup>30</sup>University of Alcalá UAH. <sup>31</sup>Port d'Informació Científica. <sup>32</sup>University of Rijeka, Department of Physics. <sup>33</sup>Institute for Theoretical Physics and Astrophysics, Universität Würzburg. <sup>34</sup>Institut für Theoretische Physik, Lehrstuhl IV: Plasma-Astroteilchenphysik, Ruhr-Universität Bochum. <sup>35</sup>INFN Sezione di Roma La Sapienza. <sup>36</sup>ILANCE, CNRS. <sup>37</sup>Physics Program, Graduate School of Advanced Science and Engineering, Hiroshima University. <sup>38</sup>INFN Sezione di Roma Tor Vergata. <sup>39</sup>Faculty of Physics and Applied Informatics, University of Lodz. <sup>40</sup>University of Split, FESB. <sup>41</sup>Department of Physics, Yamagata University. <sup>42</sup>Josip Juraj Strossmayer University of Osijek, Department of Physics. <sup>43</sup>INFN Dipartimento di Scienze Fisiche e Chimiche - Università degli Studi dell'Aquila and Gran Sasso Science Institute. <sup>44</sup>Yukawa Institute for Theoretical Physics, Kyoto University. <sup>45</sup>FZU - Institute of Physics of the Czech Academy of Sciences. <sup>46</sup>Astronomical Institute of the Czech Academy of Sciences. <sup>47</sup>Faculty of Science, Ibaraki University. <sup>48</sup>Faculty of Science and Engineering, Waseda University. <sup>49</sup>Institute of Particle and Nuclear Studies, KEK (High Energy Accelerator Research Organization). <sup>50</sup>INFN Sezione di Trieste and Università degli Studi di Trieste. <sup>51</sup>INFN and Università degli Studi di Siena, Dipartimento di Scienze Fisiche, della Terra e dell'Ambiente (DSFTA). <sup>52</sup>Escuela Politécnica Superior de Jaén, Universidad de Jaén. <sup>53</sup>Saha Institute of Nuclear Physics. <sup>54</sup>Institute for Nuclear Research and Nuclear Energy, Bulgarian Academy of Sciences. <sup>55</sup>Dipartimento di Fisica e Chimica 'E. Segrè' Università degli Studi di Palermo. <sup>56</sup>Grupo de Electronica, Universidad Complutense de Madrid. <sup>57</sup>Hiroshima Astrophysical Science Center, Hiroshima University. <sup>58</sup>School of Allied Health Sciences, Kitasato University. <sup>59</sup>RIKEN, Institute of Physical and Chemical Research. <sup>60</sup>Laboratory for High Energy Physics, École Polytechnique Fédérale. <sup>61</sup>Charles University, Institute of Particle and Nuclear Physics. <sup>62</sup>Division of Physics and Astronomy, Graduate School of Science, Kyoto University. <sup>63</sup>Institute for Space-Earth Environmental Research, Nagoya University. <sup>64</sup>Kobayashi-Maskawa Institute (KMI) for the Origin of Particles and the Universe, Nagoya University. <sup>65</sup>Graduate School of Technology, Industrial and Social Sciences, Tokushima University. <sup>66</sup>INFN Dipartimento di Scienze Fisiche e Chimiche - Università degli Studi dell'Aquila and Gran Sasso Science Institute. <sup>67</sup>Department of Physical Sciences, Aoyama Gakuin University. <sup>68</sup>IRFU, CEA, Université Paris-Saclay. <sup>69</sup>Department of Astronomy, University of Geneva. <sup>70</sup>Graduate School of Science and Engineering, Saitama University. <sup>71</sup>Institute of Space Sciences (ICE-CSIC), and Institut d'Estudis Espacials de Catalunya (IEEC), and Institutio Catalana de Recerca i Estudis Avançats (ICREA). <sup>72</sup>Dipartimento di Fisica - Università degli Studi di Torino. <sup>73</sup>Department of Physics, Konan University.